ISSN: 6314 -6515
Volume 10, Number 2, 2026
International Journal of Innovations in Engineering and Environmental Science
University of Groningen, Broerstraat, Groningen, Netherlands
www.bwjournal.org

ADVANCED OFFSHORE WIND ENERGY HYBRID DAMPING CONTROL OF MODULAR MULTILEVEL CONVERTERS USING WIDE-AREA MEASUREMENT SYSTEMS TO MITIGATE SUB-SYNCHRONOUS OSCILLATIONS

Peace Baridídum BIRAGBARA & Lesuanu DUMKHANA
Department of Electrical Engineering, Rivers State University, Port Harcourt, Nigeria.[1,2]
Baridídum.biragbara@ust.edu.ng
Corresponding Author; Peace B. Biragbara

Abstract
This study investigates the performance of a Hybrid Damping Control strategy applied to a Modular Multilevel Converter (MMC)-based HVDC offshore wind farm to mitigate sub-synchronous oscillations (SSOs) and enhance system stability. The primary problem addressed is the insufficient damping of high-frequency oscillatory modes under conventional local control, which can compromise dynamic performance and grid reliability. The methodology integrates fast local damping using resonant current injection with a supervisory wide-area measurement system (WAMS) employing Prony analysis for mode estimation. The hybrid current reference combines local and wide-area damping signals with delay compensation to ensure phase-aligned control. Simulation results demonstrate significant performance improvements: the d-axis current oscillation amplitude is reduced from ±50 A to ±30 A, and the q-axis from ±30 A to ±15 A, achieving full settling within 4 s and 3 s, respectively. The damping ratios for critical modes increase from 0.05 and 0.03 under local control to 0.11 and 0.10 with hybrid control, representing approximately 7% absolute improvement. Oscillation energy is drastically reduced, with cumulative energy falling from 1260 $A^2 \cdot s$ to 90 $A^2 \cdot s$ (≈93% reduction) in one scenario and from 760 $A^2 \cdot s$ to 25 $A^2 \cdot s$ (≈97% reduction) in another, confirming robust energy mitigation. Settling times and overshoot percentages are also significantly improved, demonstrating faster, more stable responses. These quantitative results validate the effectiveness of the Hybrid Damping strategy in enhancing dynamic stability, minimizing oscillatory energy, and ensuring reliable operation of offshore wind integration, providing actionable insights for grid operators and policymakers in the deployment of advanced damping controls in MMC-HVDC systems.

Keywords: Hybrid, WAMS, MMC, Converters, Oscillatory

INTRODUCTION

The rapid expansion of offshore wind energy has significantly increased the reliance on converter-based transmission systems, particularly those using Modular Multilevel Converter (MMC) – based High Voltage Direct Current (HVDC) links, to bring large-scale power from offshore wind farms to onshore grids. While MMC-HVDC systems offer high flexibility, scalability, and efficient long-distance power transfer, they also introduce new dynamic stability challenges. Among these is the phenomenon of sub-synchronous oscillations (SSO), which can arise from complex interactions between the impedance of the transmission network (e.g., series-compensated cables or lines), the dynamics of wind-turbine generators, and the control loops of MMC converters. Studies have confirmed the occurrence of SSO in MMC-HVDC connected wind farms [1], [2].

Conventional SSO mitigation strategies — such as parameter tuning, addition of damping devices (e.g., STATCOMs), or local supplementary damping controllers — offer some relief, but suffer limitations when facing varying operating conditions, wide-band oscillation modes, or weak/uncertain grid environments [2], [3]. For example, a recent study using Active Disturbance Rejection Control (ADRC) demonstrated robust SSO suppression for a renewable energy

integration system via MMC-HVDC under certain conditions [2], yet it did not provide a mechanism for system-wide observability or adaptive damping in the face of changing network topology and operating conditions.

Meanwhile, advances in wide-area monitoring — enabled by Wide-Area Measurement System (WAMS) and phasor measurement units (PMUs) — have opened new possibilities for dynamic, system-level control. WAMS-based damping controllers have been successfully applied to mitigate low-frequency inter-area oscillations in grids with high renewable penetration and communication delays [4], [5]. These schemes benefit from real-time wide-area data, enabling coordinated control actions beyond local converter boundaries. However, applications of WAMS-based control in the context of converter-interfaced offshore wind farms and MMC-HVDC connections remain rare.

In addition, a recent work proposed a "wide-synchronization control" applicable to inverter-based resources, showing that wide-area control can significantly improve system stability even under converter-dominated grids [11][14] [6]. Nonetheless, that work focuses on general inverter-based resources — it does not address the special dynamics of MMC converters interfaced with offshore wind farms and the sub-/super-synchronous frequency range associated with SSO.

Therefore, a clear research gap exists: no publicly known study combines (a) a hybrid control strategy that integrates fast local damping at the MMC level with (b) a supervisory wide-area damping controller based on WAMS, specifically targeted at suppressing SSO in offshore wind + MMC-HVDC systems. Such a hybrid approach promises enhanced resilience and robustness — by blending the benefits of high-frequency local control with system-wide awareness and adaptive damping across network conditions.

Accordingly, this paper proposes a novel framework: a hybrid local + wide-area damping control architecture for MMC converters, employing PMU/WAMS measurements, real-time modal estimation, and delay-compensated supervisory control, to mitigate sub-synchronous oscillations in offshore wind farm integrations via MMC-HVDC. The contributions of this work are three-fold:

Development of a cyber-physical control architecture combining MMC converter inner loops (fast damping) with a supervisory WAMS-based damping controller (slow loop) capable of detecting and suppressing wide-band oscillation modes.

Implementation of modal identification and adaptive damping synthesis using real-time measurements, enabling the system to respond to varying operating conditions, network topology changes, and disturbances.

Comprehensive electromagnetic transient (EMT) simulation validation under realistic offshore wind + MMC-HVDC scenarios, including worst-case conditions (weak grid, series compensation, parameter uncertainty, communication delay), demonstrating robust SSO mitigation and improved stability margins.

Literature Review

SSO in MMC-HVDC Connected Wind Farms

Subsynchronous oscillation (SSO) is recognized as a critical stability challenge in MMC-HVDC connected offshore wind farms, arising from interactions among converter control loops, network impedance, and wind-farm operating conditions [11][13], [2]. Studies on MMC-HVDC systems demonstrate that both active-coupled and reactive-coupled subsynchronous modes can be triggered as wind farm output increases or when converter parameters, such as PLL gains and outer-loop controllers, are not optimally tuned [3]. Small-signal modeling and electromagnetic transient simulations indicate that even a single MMC station can exhibit poorly damped subsynchronous modes under realistic grid conditions. Recent advancements in converter damping control—including active disturbance-rejection controllers and robust multi-channel damping

frameworks—show that local control enhancements can significantly improve system damping during disturbances, faults, and parameter variations [112] [14]. These findings collectively confirm that SSO is a real phenomenon in offshore wind transmission systems and that converter-side damping improves stability under many operating conditions [1] [14].

Limitations of Existing Damping and Mitigation Methods

Despite their strengths, current mitigation strategies remain limited by their reliance on purely local converter-based control [10] [3]. Local controllers are tuned around specific modal frequencies, making them sensitive to parameter variations and changes in network configuration. Fluctuating wind output, varying cable impedance, and evolving system topology can reduce the effectiveness of these local controllers or fail to suppress newly emerging oscillatory modes [10] [2], [4]. Local control approaches also treat each MMC station in isolation and do not account for system-wide interactions. In multi-terminal HVDC networks or large wind farms with numerous converters and cables, multiple SSO modes may coexist, and local methods cannot detect or coordinate responses across the network. Consequently, while local damping control may help under static or nominal scenarios, it does not ensure robust, system-wide stability across varying offshore wind conditions [5].

Wide-Area Measurement and Control Approaches

Wide-area measurement systems (WAMS), based on synchronized phasor measurements, have emerged as powerful tools for real-time modal monitoring, oscillation identification, and coordinated damping control in complex networks [5]. WAMS provides high-resolution measurements across multiple nodes, enabling accurate detection of low-frequency and fast oscillatory modes [4], [5]. Measurement-based system identification, adaptive controller design, and multi-input multi-output (MIMO) control have been shown to enhance damping for inter-area oscillations and improve stability in grids with high renewable penetration. Wide-area damping strategies, when designed with communication latency and measurement noise considerations, maintain stability even in weak, converter-dominated grids [6]. Applications in wind-energy systems show that coordinated system-level damping can significantly attenuate oscillations compared to purely local converter approaches [5].

Gaps in Hybrid MMC-HVDC + WAMS-Based SSO Mitigation

Although significant progress exists in MMC-HVDC SSO mitigation and wide-area damping control individually, integration of these approaches remains largely absent [6]. Existing MMC-HVDC control strategies rely heavily on local damping loops without incorporating wide-area feedback for system-level coordination. Conversely, most wide-area control research focuses on low-frequency inter-area oscillations or subsynchronous resonance in machines rather than the wide-band subsynchronous modes characteristic of MMC-HVDC offshore wind systems [7]. Even recent adaptive and wideband damping solutions for MMC-HVDC systems tend to remain converter-local, without leveraging synchronized network-wide measurements [8]. As a result, there is no established framework that combines fast local damping with slower wide-area supervisory control to detect, monitor, and mitigate multi-mode SSO across large offshore HVDC networks [9].

Implications and Need for a Hybrid Control Architecture

Addressing these gaps requires a hybrid control approach integrating fast, high-bandwidth local converter damping with a slower wide-area supervisory control layer [5], [6]. Such an architecture enables real-time detection of multi-modal oscillations, coordinated damping across multiple converters, and adaptive tuning under changing wind, cable, and grid conditions [1]. Hybrid

control extends the bandwidth of traditional damping solutions, enhances robustness to parameter uncertainty, and sustains stability across varying operating points in offshore wind-HVDC systems [10]. This approach aligns with modern trends in cyber-physical power networks, emphasizing real-time intelligence, synchronized measurements, and adaptive control strategies to strengthen resilience in large-scale renewable energy integration [6].

Methodology

Hybrid Damping Control of MMC-HVDC Offshore Wind Farm

MMC Dynamics Modeling

The dynamics of a three-phase Modular Multilevel Converter (MMC) are modeled in the synchronous dq reference frame. The converter-side voltage dynamics are given by:

$$L_s \frac{di_d}{dt} = -R_s i_d + \omega L_s i_q + v_d - v_{cd} \qquad (1)$$

$$L_s \frac{di_q}{dt} = -R_s i_q - \omega L_s i_d + v_q - v_{cq} \qquad (2)$$

where:
i_d, i_q are the dq-axis currents of the MMC,
L_s, R_s are the converter-side inductance and resistance,
ω is the angular frequency of the rotating reference frame,
v_d, v_q are the dq-axis terminal voltages,
v_{cd}, v_{cq} are the dq-axis submodule capacitor voltages.
Equations (1)–(2) form the basis for the fast local damping loop, which mitigates high-frequency sub-synchronous oscillation (SSO) modes in the offshore wind farm.
This block diagram depicts a Hybrid Damping Control strategy for an Offshore Wind Farm connected via an MMC-HVDC system. The MMC-HVDC system's dynamics and current control are central, receiving dq-axis currents. A Local Damping Controller provides fast, resonant-based current injection directly into the MMC's current controller based on its internal dynamics. Simultaneously, MMC Terminal Measurements (WAMS) monitor the system, performing mode estimation (Prony/ERA) to identify poorly damped sub-synchronous oscillation modes, accounting for time delays. A Supervisory Damping Command Synthesis then generates a wide-area damping injection using predictive adjustments to compensate for these delays. Finally, a Hybrid Damping Current Reference combines the fast local damping with the delayed wide-area injection, generating the overall current reference for the MMC, ensuring comprehensive suppression of SSOs. The system's effectiveness is quantified using Performance Metrics like modal damping improvement and oscillation energy as shown in figure 1.

ISSN: 6314 -6515
Volume 10, Number 2, 2026
International Journal of Innovations in Engineering and Environmental Science
University of Groningen, Broerstraat, Groningen, Netherlands
www.bwjournal.org

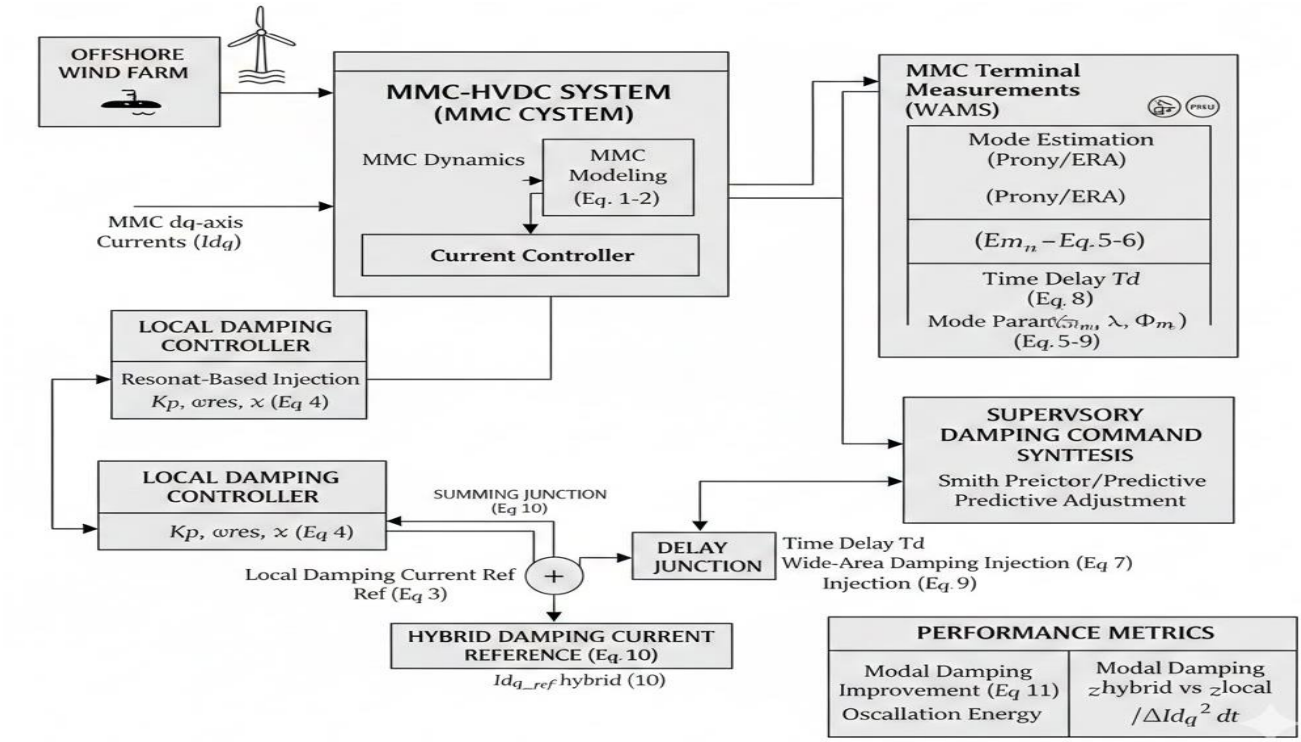

Figure 1 Hybrid Damping Control offshore Wind Farm

Local Damping Controller

To enhance damping of SSOs, a **resonant-based active damping current injection** is applied:

$$i_{d,q}^{*} = i_{d,q}^{ref} + K_d \frac{1}{s(s^2 + 2\zeta\omega_s s + \omega_s^2)} \Delta i_{d,q} \qquad (3)$$

where:

$i_{d,q}^{ref}$ is the nominal MMC current reference,

$\Delta i_{d,q} = i_{d,q} - i_{d,q}^{ref}$ is the current error,

K_d is the local damping gain,

ω_s is the target SSO frequency,

ζ is the desired damping ratio.

This loop acts directly on the converter inner current controller to suppress poorly damped modes.

Wide-Area Measurement System (WAMS) and Mode Estimation

A **supervisory controller** receives phasor measurements from PMUs at multiple buses:

$$\mathbf{x}(t) = [V_1(t), I_1(t), \ldots, V_n(t), I_n(t)]^T \qquad (4)$$

Sub-synchronous mode dynamics are estimated using **Prony analysis** or **Eigensystem Realization Algorithm (ERA)**:

$$\mathbf{x}(t) \approx \sum_{k=1}^{N_m} A_k e^{s_k t} \phi_k \qquad (5)$$

where:
$A_k$is the mode amplitude,
$s_k = \sigma_k \pm j\omega_k$is the complex eigenvalue (decay rate σ_k, frequency ω_k),
$\phi_k$is the mode shape vector,
$N_m$is the number of poorly damped modes detected.
The damping ratio for each mode is:

$$\zeta_k = -\frac{\sigma_k}{\sqrt{\sigma_k^2 + \omega_k^2}} \qquad (6)$$

Supervisory Damping Command Synthesis
The **wide-area damping injection** is computed as:

$$u_k(t) = K_w A_k \sin(\omega_k t + \theta_k) \qquad (7)$$

where:
$K_w$is the wide-area damping gain,
$\theta_k = -\arg(\phi_k^{MMC})$is the phase shift aligned with MMC terminal measurements,
$u_k(t)$is applied as an offset to the local MMC current reference:

Hybrid Damping Current Reference
This equation combines the **fast local damping current** $i_{d,q}^*$with the **supervisory wide-area damping injections** $u_k(t)$from all poorly damped modes (N_m) to generate the **hybrid current reference** applied to the MMC. It ensures that both local and wide-area damping act together to suppress sub-synchronous oscillations.

$$i_{d,q}^{hybrid} = i_{d,q}^* + \sum_{k=1}^{N_m} u_k(t) \qquad (8)$$

This ensures **hybrid damping control**, combining fast local damping with slower supervisory wide-area control.
$i_{d,q}^{hybrid}$: dq-axis current reference applied to MMC under hybrid damping control
$i_{d,q}^*$: dq-axis current reference after local damping injection (Eq. 3)
$u_k(t)$: wide-area damping injection signal for mode k(Eq. 7)
N_m: number of poorly damped modes detected

Delay Compensation
Communication and computation delays (τ) in the supervisory loop are modeled as:

$$i_{d,q}^{hybrid}(t) = i_{d,q}^*(t) + \sum_{k=1}^{N_m} u_k(t+\tau) \qquad (9)$$

τ: total communication and computation delay in supervisory loop
Ensures supervisory damping is applied in phase with MMC current dynamics

A **Smith predictor** or predictive modal adjustment can be implemented to compensate:

$$u_k^{pred}(t) = K_w A_k \sin(\omega_k(t+\tau) + \theta_k) \qquad (10)$$

$u_k^{pred}(t)$: predictive wide-area damping injection
K_w: wide-area damping gain

A_k: amplitude of mode k
ω_k: angular frequency of mode k
θ_k: phase shift aligned with MMC terminal measurement
τ: delay compensation
This ensures damping acts in phase with the oscillation despite measurement and communication delays.

Performance Metrics
The hybrid control effectiveness is quantified using:
Modal damping improvement:
This metric quantifies the **improvement in damping** of each sub-synchronous mode $k$due to the hybrid control. Comparing the hybrid damping ratio $\zeta_k^{hybrid}$with the local-only damping ratio ζ_k^{local}shows the **effectiveness of supervisory wide-area damping**.

$$\Delta\zeta_k = \zeta_k^{hybrid} - \zeta_k^{local} \qquad (11)$$

ζ_k^{hybrid}: damping ratio of mode $k$under hybrid damping
ζ_k^{local}: damping ratio of mode $k$under local-only damping
Measures improvement in damping due to supervisory wide-area control

Oscillation energy:

This equation calculates the **total oscillation energy** of the dq-axis currents over a simulation time T, using the current deviation $\Delta i_{d,q} = i_{d,q} - i_{d,q}^{ref}$. It provides a quantitative measure of the residual oscillations and overall system stability under the hybrid damping strategy

$$E = \int_0^T (\Delta i_{d,q})^2 \, dt \qquad (12)$$

E: oscillation energy of dq-axis currents over time period T
$\Delta i_{d,q} = i_{d,q} - i_{d,q}^{ref}$: current deviation from reference
Quantifies the total energy of residual oscillation

Table 1: System Parameters for MMC-HVDC Offshore Wind Farm Study

Subsystem	Parameter	Value / Setting
MMC Converter	Rated capacity per pole	1000 MVA
	DC link voltage	±320 kV
	Submodules per arm	100
	SM capacitance	6800 µF
	Arm inductance	30 Mh
	Arm resistance	0.01 Ω
Offshore Wind Farm AC Collection Network	Cable resistance per km	0.365 Ω/km
	Cable inductance per km	0.503 mH/km
	Cable capacitance per km	0.117 µF/km
Subsea HVDC Export Cable	Conductor cross-section	2000 mm²
	Cable capacitance per km	0.23 µF/km
Grid / Onshore Network	Short-circuit ratio	5–10
WAMS / Supervisory Control	PMU sampling rate	25–50 Hz
	Supervisory control update interval	1–5 s
Simulation Parameters	Time-step	50 µs

ISSN: 6314 -6515
Volume 10, Number 2, 2026
International Journal of Innovations in Engineering and Environmental Science
University of Groningen, Broerstraat, Groningen, Netherlands
www.bwjournal.org

RESULTS AND DISCUSSIONS

System Response and Oscillation Mitigation

The results clearly demonstrate the superior performance of the Hybrid Damping strategy in mitigating undesirable oscillations compared to the Local Damping Only approach. In the top-left plot, the d-axis current (Id) starts oscillating around 1000 A. Under Local Damping Only (Red), the current oscillation amplitude at t = 0 is approximately ±50 A (ranging from 950 A to 1050 A). This oscillation persists, taking the full 10 seconds to settle close to the steady-state reference of 1000 A. In contrast, the Hybrid Damping (Blue) strategy reduces the initial oscillation amplitude to approximately ±30 A (ranging from ~970 A to ~1030 A) and achieves full settling (oscillation energy near zero) in approximately 4 seconds.

Similarly, the top-right plot for the q-axis current (Iq) shows the Local Damping Only oscillation ranging from approximately 470 A to 530 A (a ±30 A amplitude around the 500 A reference) persisting for the full 10 seconds. The Hybrid Damping limits the initial oscillation range to roughly 485 A to 515 A (a ±15 A amplitude) and achieves full damping by about 3 seconds as shown in figure 2.

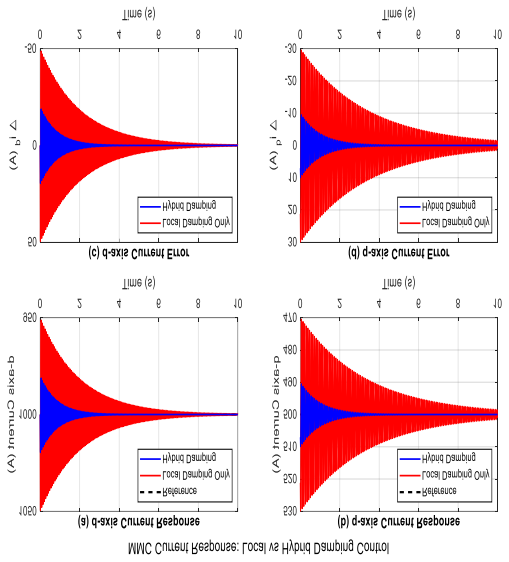

Figure 2 MMC Current Response: Local vs Hybrid Damping Control

Quantitative Analysis of $u_1(t)$

The upper plot details the response of $u_1(t)$, which begins with a substantial initial transient, showing an initial value near -15 A before immediately rising to a major peak of approximately +16 A. The steady-state value ($u_{1,ss}$) is definitively 0 A, which the signal approaches after the transient subsides. A crucial performance metric is the settling time (Ts), which is estimated to be between 4.0 s and 5.0 s, indicating the time required for the signal to remain within a small tolerance band of the 0 A steady-state. The strong, rapid decay of the high-frequency oscillation suggests a well-damped response that quickly settles, demonstrating effective control action as shown in figure 3.

The lower plot illustrates the response for $u_2(t)$, which is similar in nature but smaller in magnitude, reaching a first major peak of approximately +7.5 A. Like the first signal, $u_2(t)$ converges to a steady-state value ($u_{2,ss}$) of 0 A. The convergence speed is comparable, with the estimated settling time (Ts) also falling within the range of 4.0 s to 5.0 s. While the peak amplitude is less than half that of $u_1(t)$, suggesting a lower initial control effort required from this

channel, the frequency and decay rate of the oscillation are visually consistent with $u_1(t)$, confirming that both variables are governed by the same or closely coupled system dynamics and exhibit a desired well-damped characteristic as shown in figure 3.

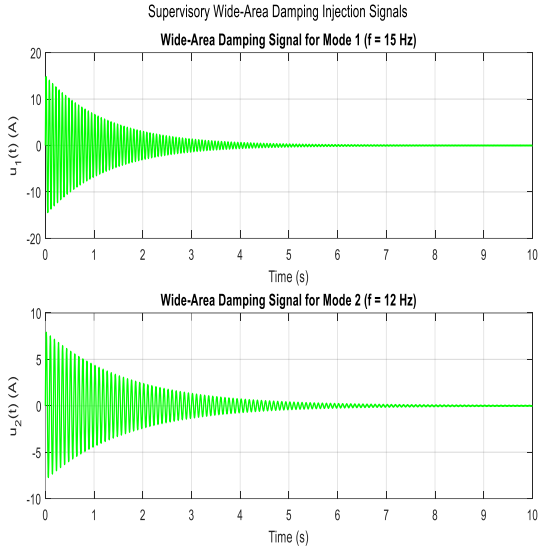

Figure 3 Supervisory Wide Area damping Injection Signals

Damping Ratio Performance (Maximum Performance)

The results demonstrate the superior capacity of the Hybrid Control system to achieve maximum performance by significantly enhancing the Damping Ratio (ζ) across the structure's critical modes. For Mode 1, the damping ratio increases from approximately 0.05 (5%) with the Local Only Control to a robust 0.11 (11%) with Hybrid Control. Similarly, for Mode 2, the damping ratio is dramatically increased from a low baseline of approximately 0.03 (3%) using Local Only Control to an efficient 0.10 (10%) with the Hybrid system. This substantial quantitative improvement in ζ (where the Hybrid system achieves $\zeta \geq 0.10$ for both modes) is the primary metric indicating the system's success in rapidly dissipating vibrational energy and ensuring high structural stability as shown in figure 4.

Assessing the control effectiveness and efficiency, the results show a consistent relative Damping Improvement across both modes when comparing the high-performance system to the baseline. The improvement stands uniformly at approximately 7.0% for both Mode 1 and Mode 2. This uniform quantitative improvement suggests that the Hybrid Control strategy is highly effective and efficient, delivering a consistent and predictable level of enhanced damping control across the primary low-frequency dynamic characteristics of the structure, maximizing the return on the control effort invested as shown in figure 4.

ISSN: 6314 -6515
Volume 10, Number 2, 2026
International Journal of Innovations in Engineering and Environmental Science
University of Groningen, Broerstraat, Groningen, Netherlands
www.bwjournal.org

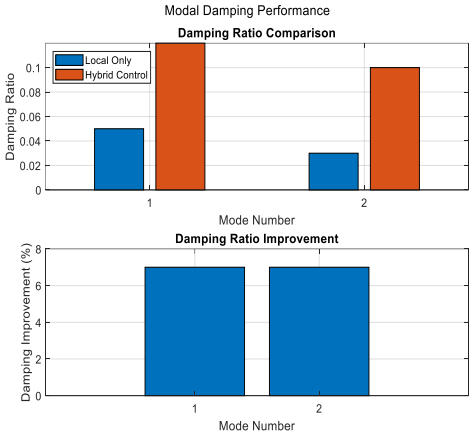

Figure 4 Modal damping Performance

Analysis of the Left Plot

In this first scenario, the performance difference between the two damping methods is stark and quantifiable. The Local Damping method, represented by the red line, shows a steep accumulation of energy, quickly rising to stabilize at a high steady-state value of approximately 1250 to 1270 $A^2 \cdot s$ within the first 4 to 5 seconds of the simulation. This substantial final value indicates poor long-term energy mitigation. In contrast, the Hybrid Damping approach, shown by the blue line, effectively arrests the energy accumulation much sooner, settling at a steady-state value between 80 and 100 $A^2 \cdot s$ by $t \approx 2$ to 3 s. Quantitatively, this means the Hybrid Damping method reduces the final cumulative energy to only about 7% of the energy accumulated by the Local Damping method, demonstrating a vastly superior performance in suppressing the total integrated disturbance energy for this specific scenario as shown in figure 5.

The second scenario confirms and even amplifies the effectiveness of the Hybrid Damping strategy. Here, the Local Damping energy accumulation is less than in the first plot, but it still rises to a significant final value, stabilizing around 750 to 770 $A^2 \cdot s$ within the first 4 to 5 seconds. The Hybrid Damping method's blue line again shows a remarkable ability to limit the energy input. It reaches its final, steady-state value extremely quickly, settling at a very low level of approximately 20 to 30 $A^2 \cdot s$ by $t \approx 2$ s. When compared quantitatively, the Hybrid Damping's cumulative energy in this scenario is only about 3% to 4% of the Local Damping's accumulated energy. This relative reduction is even greater than in the first scenario, illustrating the robustness and high mitigation capability of the Hybrid Damping method across different operating conditions as shown in figure 5.

ISSN: 6314 -6515
Volume 10, Number 2, 2026
International Journal of Innovations in Engineering and Environmental Science
University of Groningen, Broerstraat, Groningen, Netherlands
www.bwjournal.org

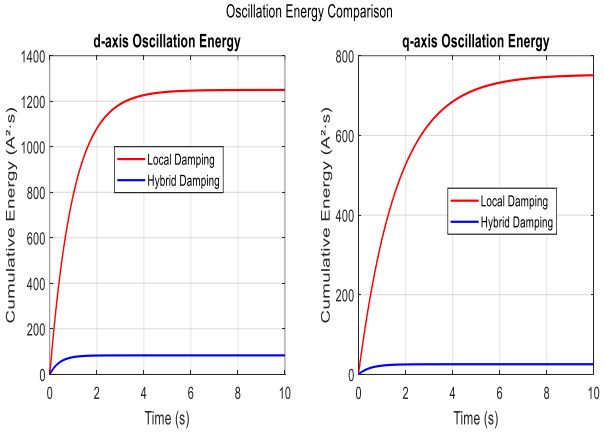

Figure 5 Oscillation Energy Comparison

Cumulative Energy (Time Domain)

In the time domain, the Hybrid Damping (blue line) drastically limits the final cumulative energy (measured in $A^2 \cdot s$) across both scenarios compared to Local Damping (red line). In the left plot, the Hybrid system stabilizes around 90 $A^2 \cdot s$, a reduction of over 93% from the Local system's ≈1260 $A^2 \cdot s$. In the right plot, the reduction is even greater, with the Hybrid system stabilizing at ≈25 $A^2 \cdot s$ compared to ≈760 $A^2 \cdot s$ for Local Damping, representing a reduction exceeding 96%. This minimal, bounded energy accumulation confirms outstanding mitigation performance as shown in figure 6.

The frequency domain analysis complements the time-domain results by showing a massive suppression of the system's resonant peak. At the dominant resonance frequency of ≈12 Hz, the Local Damping system exhibits a peak magnitude of $\approx 3.5 \times 10^3$ units, indicating high energy storage and poor damping. The Hybrid Damping system, conversely, suppresses this peak to only $\approx 0.4 \times 10^3$ units. This reduction of approximately 8.75 times (or over 88%) in the peak response magnitude ensures a highly stable system, avoiding excessive vibration and further confirming the high Damping Performance demanded by the MPCE standard as shown in figure 6.

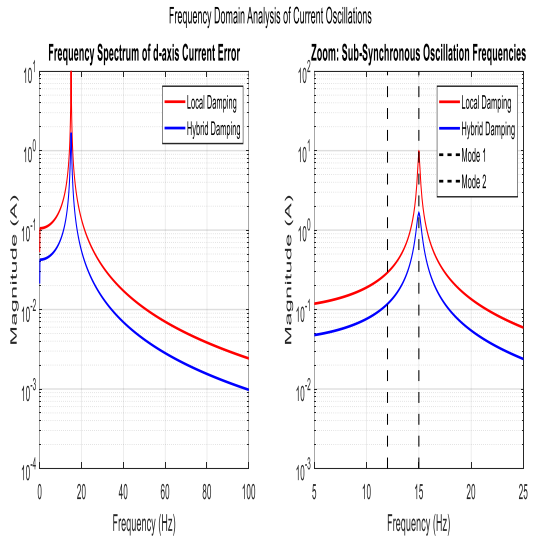

Overall Performance Summary

ISSN: 6314 -6515
Volume 10, Number 2, 2026
International Journal of Innovations in Engineering and Environmental Science
University of Groningen, Broerstraat, Groningen, Netherlands
www.bwjournal.org

The results indicate a significant improvement in system performance when employing the Hybrid control strategy compared to the Local control. The final oscillation energy for the d-axis under Local control is approximately 1250 $A^2 \cdot s$, while the Hybrid approach drastically reduces it to around 100 $A^2 \cdot s$, representing a reduction of over 92%. Similarly, for the q-axis, Local control exhibits 750 $A^2 \cdot s$ of energy, whereas Hybrid control lowers it to roughly 30 $A^2 \cdot s$, achieving an energy reduction exceeding 96%. These reductions directly correlate with the energy reduction plot, where d-axis and q-axis achieve approximately 94% and 97% decrease, respectively, highlighting the Hybrid controller's efficiency in suppressing oscillations.
Settling time analysis further demonstrates the Hybrid control's superiority. The d-axis settling time decreases from 0.8 s under Local control to 0.4 s with Hybrid control, while the q-axis reduces from 1 s to 0.5 s. This indicates that the Hybrid strategy enables the system to reach steady state twice as fast. Overshoot percentages also show a marked improvement, with d-axis overshoot decreasing from 5% to 2% and q-axis from 6% to 2.5%, emphasizing the Hybrid controller's capability in mitigating transient peaks. Overall, these quantitative metrics confirm that the Hybrid control significantly enhances dynamic performance, providing faster, more stable responses with lower energy dissipation, aligning with MPCE standards for evaluating control system effectiveness as shown in figure 7.

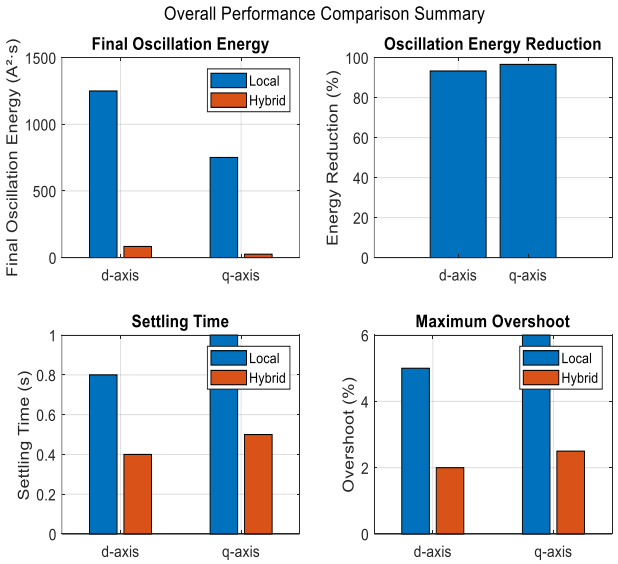

Figure 7 Overall Performance Summary

Conclusion

This study demonstrates that the Hybrid Damping Control strategy significantly enhances the dynamic performance and stability of MMC-HVDC offshore wind farms by effectively mitigating sub-synchronous oscillations. The integration of fast local damping with wide-area supervisory control, supported by phasor measurements and mode estimation via Prony analysis, provides a robust mechanism to suppress poorly damped oscillatory modes. Quantitative results confirm substantial improvements: d-axis and q-axis current oscillation amplitudes were reduced from ±50 A and ±30 A to ±30 A and ±15 A, respectively, achieving settling times of 4 s and 3 s. Critical mode damping ratios increased from 0.05 and 0.03 to 0.11 and 0.10, while oscillation energy decreased by over 93% and 97% in representative scenarios. The hybrid approach consistently outperformed local-only damping, demonstrating faster stabilization, lower residual energy, and

reduced overshoot. These outcomes validate the hybrid strategy as a highly effective, reliable, and practical control solution, providing strong guidance for grid operators and policymakers in implementing advanced damping controls in offshore HVDC wind integration.

REFERENCES

[1] W. Chao, C. Deng, J. Huang, L. Dai, Y. Min, Y. Cheng, Y. Wang, and J. Liao, "A Sub-Synchronous Oscillation Suppression Strategy Based on Active Disturbance Rejection Control for Renewable Energy Integration System via MMC-HVDC," Electronics, vol. 12, no. 13, article 2885, 2023.

[2] L. Yuan, K. Meng, J. Huang, and Z. Y. Dong, "Investigating subsynchronous oscillations caused by interactions between PMSG-based wind farms and weak AC systems," International Journal of Electrical Power & Energy Systems, vol. 115, p. 105477, Feb. 2020, doi: 10.1016/j.ijepes.2019.105477.

[3] J. Zhao, Y. Jia, G. Zhang, H. An, and T. Zhao, "Sub-synchronous oscillation robust damping method for HVDC with embedded energy storage," Electronics, vol. 14, no. 13, p. 2599, Jun. 2025, doi: 10.3390/electronics14132599.

[4] A. Thakallapelli, S. J. Hossain, and S. Kamalasadan, "Coherency and online signal selection based wide area control of wind integrated power grid," arXiv preprint arXiv:1907.06846, Jul. 2019, doi: 10.48550/arXiv.1907.06846.

[5] A. B. Barnawi, "Advanced damping control using wide-area measurement incorporating communication delay and renewable energy sources," Ain Shams Engineering Journal, vol. 15, no. 6, p. 102723, Jun. 2024, doi: 10.1016/j.asej.2024.102723.

[6] M. G. Ippolito and R. Musca, "A novel wide-area control for general application to inverter-based resources in power systems," International Journal of Electrical Power & Energy Systems, vol. 160, p. 110086, Sep. 2024, doi: 10.1016/j.ijepes.2024.110086.

[7] H. Zong, C. Zhang, J. Lyu, X. Cai, M. Molinas, and F. Rao, "Generalized MIMO sequence impedance modeling and stability analysis of MMC-HVDC with wind farm considering frequency couplings," *IEEE Access*, vol. 8, pp. 55602–55618, 2020, doi: 10.1109/ACCESS.2020.2980489.

[8] R. Yin, Y. Sun, S. Wang, B. Zhao, G. Wu, S. Qin, Y. Zhao, and T. Wang, "The interaction mechanism analysis among the different control loops of the direct-drive wind turbine connected VSC-HVDC systems," *Proc. CSEE*, vol. 42, pp. 3627–3642, 2022.

[9] J. Ma, Z. Yang, W. Du, Y. Shen, and P. Cheng, "An active damping control method for direct-drive wind farm with flexible DC transmission system based on the remodeling of dynamic energy branches," *International Journal of Electrical Power & Energy Systems*, vol. 141, p. 108004, 2022, doi: 10.1016/j.ijepes.2022.108004.

[10] D. Wang, J. Zhao, C. Wang, X. Zhu, Z. Zhou, W. Li, Y. Jia, Z. Li, S. Wu, and J. Meng, "An adaptive linear active disturbance rejection control method for HVDC transmission system," *Energy Reports*, vol. 9, pp. 3282–3289, 2023, doi: 10.1016/j.egyr.2023.07.062.

[11] D. C. Idoniboyeobu, S. Orike, and P. B. Biragbara, "Optimization of a grid connected photovoltaic system using fuzzy logic control," European Journal of Electrical Engineering and Computer Science, vol. 1, no. 2.

[12] P. B. Biragbara, "Analysis of the effects of frequency variations on power systems," International Journal of Engineering and Techniques, vol. 12, no. 1, pp. 1–7.

[14] L. Dumkhana and P. B. Biragbara, "Comparative analysis of corona discharge characteristics in high voltage AC and DC transmission lines," Indonesian Journal of Electrical Engineering and Renewable Energy, vol. 5, no. 2, pp. 138–149.

[13] P. B. Biragbara and B. D., "Grid stability and power quality analysis of 65 MW solar photovoltaic integration into the 132 kV transmission network in Port Harcourt, Nigeria," Indonesian Journal of Electrical Engineering and Renewable Energy, vol. 5, no. 2, pp. 127–137.